International Journal of Innovative
Computing, Information and Control
Volume **15**, Number **3**, June **2019**

ICIC International ©2019 ISSN 1349-4198
pp. **891–904**

AN IMPROVED BACKSTEPPING SLIDING MODE CONTROL FOR POWER SYSTEMS WITH SUPERCONDUCTING MAGNETIC ENERGY STORAGE SYSTEM

Adirak Kanchanaharuthai[1] and Ekkachai Mujjalinvimut[2]

[1]Department of Electrical Engineering
Rangsit University
52/347 Muang-Ake, Phaholyothin Rd., Lak-Hok, Muang, Patumthai 12000, Thailand
adirak@rsu.ac.th

[2]Department of Electrical Engineering
Faculty of Engineering
King Mongkut's University of Technology Thonburi
Pracha Uthit Road, Bang Mod, Bangkok 10140, Thailand
ekkachai.muj@kmutt.ac.th

Received July 2018; revised November 2018

Abstract. *In this paper, an improved backstepping sliding mode controller is presented for stabilizing an electric power system including a superconducting magnetic energy storage (SMES) system. In the first two steps of the design procedure, a feedback stabilizing control law is designed through improved backstepping strategy while a sliding mode surface is included in the final step. The resulting control law is employed not only to enhance transient stability and voltage regulation of the system including SMES device, but also to ensure the overall closed-loop system stability. The developed control law is evaluated on a single-machine infinite bus (SMIB) power system with SMES. The simulation results are used to demonstrate the performance of the designed scheme compared with that of a conventional backstepping control and an immersion and invariance (I&I) control. From the simulation, the proposed method has dynamic performances almost equal to the I&I one. Further, it is capable of improving both transiently stability and the dynamic properties better than the conventional backstepping method in spite of the presence of a large disturbance or a small disturbance.*

Keywords: Backstepping sliding mode method, Nonlinear control, SMES, Transient stabilization

1. **Introduction.** In recent years, there are a number of researches focusing on the use of the energy storage system such as superconducting magnetic energy storage (SMES), flywheel energy storage system (FESS), battery energy storage system (BESS) [1-6] to improve power system stability and operation. In particular, they have shown the feasibility and effectiveness of energy storage to enhance transient stability and to damp power system oscillation. Consequently, considerable attention has been paid for the use of energy storage devices due to their ability to further enhance power transfer capability and to augment both small-signal and transient stability in the power systems. Among a family of energy storage technologies, a device of our particular interest is the superconducting magnetic energy storage (SMES) in this paper because of its ability to inject and absorb active and reactive power. Also, it is able to provide benefit to a lot of potential utility applications [2] such as system stability, bulk energy management, transient voltage

DOI: 10.24507/ijicic.15.03.891

dip improvement, automatic generation control, wind generator stabilization, and power quality improvement.

Until now, there has been recently considerable research addressing the application of SMES with the help of the linearization method based on small perturbation theory and linearized dynamical models. However, there is less attention that has devoted to a combination of generator excitation with SMES based on nonlinear control strategy [5-12]. Wang et al. [5] developed an adaptive nonlinear control strategy for synchronous generators with SMES unit for multi-machine power systems based on the Hamiltonian function method. In [6], a backstepping method has been extended to the non-strict feedback form of a class of nonlinear systems. The scheme is used not only to design the generator excitation and SMES controller in the SMIB model, but also to improve the power system stability such as generator terminal voltage, and the power oscillation. In [7], the authors presented a nonlinear adaptive algorithm for a power system including generator excitation, and a thyristor-controlled superconducting magnetic energy storage control to improve transient stability in spite of having unknown or varying parameters. Despite having a large disturbance, a robust nonlinear excitation and SMES controller [8] was proposed to enhance transient stability of a single-machine infinite bus (SMIB) system. A combination of the feedback linearization and linear $\mathcal{H}_\infty$ method was applied to the design of a combined generator excitation and SMES control for power systems. The strategy can achieve the desired transient stability improvement together with evaluation with experimental results as reported in [9]. A Hamiltonian function design strategy [10] was used to design a robust adaptive controller of synchronous generators with SMES for the stability improvement of power systems in the presence of external disturbances and unknown parameters. Mahmud et al. [11] developed a dynamic model of SMES based on the equivalent circuit. Afterwards, the feedback linearizing control was designed to satisfy the stability requirements and simultaneously to improve the dynamic stability.

Currently, an advanced control method, in particular, an immersion and invariance (I&I) method [12], was applied to the design of a nonlinear coordinated generator excitation and SMES controller for transient stability enhancement of power systems. Unfortunately, even if the I&I control methodology is most effective and can be applied for various types of systems [13, 14], there are a few of inevitable disadvantages. In particular, there are no systematic ways in selecting the mapping from the algebraic equation, the suitable target dynamics, and the suitable Lyapunov (energy) function. These lead to main difficulties of this I&I method. Likewise, an adaptive control design [15] based on synergetic control theory was presented to enhance power system stability; however, a suitable selection of some coefficients in a macro-variable that is used to design the desired control law is not easy, thereby resulting in instability. As a result, to overcome these difficulties, this paper deals with the design of a nonlinear controller combining both merits of backstepping control and sliding mode control as successfully applied for a variety of practical systems [16-19]. In the study, there are three steps in finding the desired control law. In the first two steps, the backstepping approach is used to select recursively the virtual control variables. In the final step, sliding mode control approach is combined to determine the control law capable of stabilizing the closed-loop system. In order to further improve the design procedure, an error compensation [20, 21] is included to compensate the dynamic impact of unknown error in the design process. Therefore, the main contributions of this work lie in the following: (i) The use of an improved backstepping sliding mode control to make the closed-loop system of power systems with SMES asymptotically stable has not been studied before; (ii) All trajectories of the overall closed-loop system are bounded and gradually return to the desired equilibrium point,

and power angle stability together with frequency and voltage regulations is simultaneously achieved; (iii) In practice, the developed control law can enhance power transfer capability, reduction of system oscillation, and boosting voltage stability together with improving voltage sag in power systems by injecting and rejecting the active power and the reactive power, simultaneously; (iv) In comparision with a conventional backstepping control and I&I control, the developed control law offers better transient control performances; and (v) The resulting control law includes the error compensation to handle the adverse effect of unknown error and has not the effect of chattering problems arising from discontinuous control signals.

The remainder of this paper is organized as follows. Simplified dynamic models of an SMIB power system with generator excitation and SMES are briefly described in Section 2. Control design procedure is given in Section 3 while the stability analysis is mentioned in Section 4. Simulation results are given in Section 5. A conclusion is stated in Section 6.

2. **Power System Models with SMES.** In this section, dynamic models of the synchronous generator and SMES are briefly provided. According to the result presented in [12], an SMIB power system with generator excitation control of a synchronous generator and SMES control can be expressed as

$$\begin{cases} \dot{\delta} = \omega - \omega_s \\ \dot{\omega} = \dfrac{1}{M}\left(P_m - P_e - P_d - P_q - D(\omega - \omega_s)\right) \\ \dot{P}_e = (-a + (\omega - \omega_s)\cot\delta)P_e + \dfrac{bV_\infty \sin 2\delta}{2X'_{d\Sigma}} + \dfrac{V_\infty \sin\delta}{X'_{d\Sigma}} \cdot \dfrac{u_f}{T'_0} \\ \dot{P}_d = \dfrac{P_d}{P_e}\dot{P}_e + \dfrac{P_e X_2 \cot\delta}{V_\infty} \cdot \dfrac{1}{T_d}\left(-\left(\dfrac{P_d V_\infty}{P_e X_2 \cot\delta} - I_{de}\right) + u_d\right) \\ \qquad + \dfrac{I_d P_e X_2}{V_\infty}(\cot^2\delta + 1)(\omega - \omega_s) \\ \dot{P}_q = \dfrac{P_q}{P_e}\dot{P}_e + \dfrac{P_e X_2}{V_\infty} \cdot \dfrac{1}{T_q}\left(-\left(\dfrac{P_q V_\infty}{P_e X_2} - I_{qe}\right) + u_q\right) \end{cases} \tag{1}$$

where δ is the power angle of the generator, ω denotes the relative speed of the generator, $D \geq 0$ is a damping constant, P_m is the mechanical input power, P_e is the electrical power, without SMES, delivered by the generator to the voltage at the infinite bus V_∞, P_d and P_q are the electrical power from SMES, ω_s is the synchronous machine speed, $\omega_s = 2\pi f$, H represents the per unit inertial constant, f is the system frequency and $M = 2H/\omega_s$. $X'_{d\Sigma} = X'_d + X_T + X_L$ is the reactance consisting of the direct axis transient reactance of SG, the reactance of the transformer, and the reactance of the transmission line X_L. Similarly, $X_{d\Sigma} = X_d + X_T + X_L$ is identical to $X'_{d\Sigma}$ except that X_d denotes the direct axis reactance of SG. T'_0 is the direct axis transient short-circuit time constant. u_f is the field voltage control input to be designed. For SMES devices, I_d and I_q denote active and reactive currents in the synchronous d-q frame. I_{de} and I_{qe} are equilibrium points of SMES currents. T_d and T_q are time constants of SMES models. u_d and u_q are the SMES control input to be designed.

In order to simplify the state-space equation of the system (1), let us introduce the vector of the state variable as $x = [x_1, x_2, x_3, x_4, x_5]^T = [\delta, \omega - \omega_s, P_e, P_d, P_q]^T$. Thus, the dynamic model of the power system with SMES can be expressed as an affine nonlinear system as follows:

$$\dot{x} = f(x) + g(x)u(x) \tag{2}$$

where

$$f(x) = \begin{bmatrix} f_1(x) \\ f_2(x) \\ f_3(x) \\ f_4(x) \\ f_5(x) \end{bmatrix} = \begin{bmatrix} x_2 \\ \dfrac{1}{M}\left(P_m - Dx_2 - x_3 - x_4 - x_5\right) \\ (-a + x_2 \cot x_1)x_3 + \dfrac{bV_\infty \sin 2x_1}{2X'_{d\Sigma}} \\ \dfrac{x_4}{x_3} f_3(x) - x_3 \tan x_1(\cot^2 x_1 + 1)x_2 - \dfrac{x_4}{T_d} + \dfrac{x_3 X_2 \cot x_1}{V_\infty T_d} I_{de} \\ \dfrac{x_5}{x_3} f_3(x) - \dfrac{x_5}{T_q} + \dfrac{x_3 X_2}{V_\infty T_q} I_{qe} \end{bmatrix}$$

$$g(x) = \begin{bmatrix} 0 & 0 & 0 \\ 0 & 0 & 0 \\ g_{31}(x) & 0 & 0 \\ g_{41}(x) & g_{42}(x) & 0 \\ g_{51}(x) & 0 & g_{53}(x) \end{bmatrix} = \begin{bmatrix} 0 & 0 & 0 \\ 0 & 0 & 0 \\ \dfrac{V_\infty \sin x_1}{X'_{d\Sigma}} & 0 & 0 \\ \dfrac{x_4 V_\infty \sin x_1}{x_3 X'_{d\Sigma}} & \dfrac{x_3 X_2 \cot x_1}{V_\infty} & 0 \\ \dfrac{x_5 V_\infty \sin x_1}{x_3 X'_{d\Sigma}} & 0 & \dfrac{x_3 X_2}{V_\infty} \end{bmatrix}, \; u(x) = \begin{bmatrix} \dfrac{u_f}{T'_0} \\ \dfrac{u_d}{T_d} \\ \dfrac{u_q}{T_q} \end{bmatrix}$$

The region of operation is defined as the set $\mathcal{D} = \left\{x \in \mathcal{S} \times \mathbb{R} \times \mathbb{R} \times \mathbb{R} \times \mathbb{R} |\ 0 < x_1 < \frac{\pi}{2}\right\}$. The open loop operating equilibrium is denoted by $x_e = [x_{1e},\ 0,\ P_{ee},\ P_{de},\ P_{qe}]^T = [x_{1e},\ 0,\ P_m,\ 0,\ 0]^T$.

For notational convenience, the system (2) can be rewritten as follows.

$$\begin{cases} \dot{x}_1 = x_2 \\ \dot{x}_2 = \dfrac{1}{M}(P_m - Dx_2 - x_3 - x_4 - x_5) \\ \dot{x}_3 = f_3(x) + g_{31}(x)\dfrac{u_f}{T'_0} \\ \dot{x}_4 = f_4(x) + g_{41}(x)\dfrac{u_f}{T'_0} + g_{42}(x)\dfrac{u_d}{T_d} \\ \dot{x}_5 = f_5(x) + g_{51}(x)\dfrac{u_f}{T'_0} + g_{53}(x)\dfrac{u_q}{T_q} \end{cases} \tag{3}$$

Thus, the objective of this paper is to solve the problem of the transient stabilization of the system (3), which can be formulated as follows: with the help of the improved backstepping sliding mode methodology, to design a stabilizing feedback controller $u(x)$ such that the resulting closed-loop system is asymptotically stable at the only equilibrium (x_e) and $x \to x_e$ as $t \to \infty$.

3. Controller Design.

In this section, with the help of the backstepping sliding mode scheme, the control law is developed step by step as follows.

Step 1: We start the backstepping sliding mode procedure by considering the first subsystem of the system (3). x_2 is regarded as the virtual control variable. Then, the virtual control of x_2 is designed as

$$x_2^* = -c_1 x_1 - p_1 e_2 \tag{4}$$

where $c_1 > 0$ is a design parameter, $0 < p_1 < 1$ is viewed as an error compensation to compensate for the dynamic impact of the unknown error in the stabilization process

[20, 21]. Let us define the error variable $e_2 = x_2 - x_2^*$ and $e_1 = x_1$. Then, we have

$$\dot{e}_1 = (1 - p_1)e_2 - c_1 e_1 \tag{5}$$

For the system (5), we choose the Lyapunov function as $V_1 = \frac{1}{2}e_1^2$. The time derivative of V_1 along the system trajectory is $\dot{V}_1 = e_1((1 - p_1)e_2 - c_1 e_1) = -c_1 e_1^2 + (1 - p_1)e_1 e_2$. It is clear that $\dot{V}_1 \leq 0$ where $e_2 = 0$.

Step 2: Let us define the augmented Lyapunov function of Step 1 as $V_2 = V_1 + \frac{1}{2}e_2^2$. Notice that

$$\dot{e}_2 = \dot{x}_2 - \dot{x}_2^* = \frac{1}{M}(P_m - Dx_2 - x_3 - x_4 - x_5) + c_1 x_2 + p_1 \dot{e}_2 \tag{6}$$

and we have

$$\dot{e}_2 = \frac{1}{1 - p_1}\left(\frac{1}{M}(P_m - Dx_2 - x_3 - x_4 - x_5) + c_1 x_2\right) \tag{7}$$

Then the time derivative of V_2 along the system trajectory is

$$\begin{aligned}\dot{V}_2 &= \dot{V}_1 + e_2\dot{e}_2 \\ &= -c_1 e_1^2 + e_2\left[(1 - p_1)e_1 + \frac{1}{1 - p_1}\left(\frac{1}{M}(P_m - Dx_2 - x_3 - x_4 - x_5) + c_1 x_2\right)\right]\end{aligned}$$

From (7), x_3, x_4 and x_5 are taken as the virtual control variables. Define the error variables $e_3 = x_3 - x_3^*$, $e_4 = x_4 - x_4^*$ and $e_5 = x_5 - x_5^*$, and then three virtual control variables are chosen as

$$\begin{cases} x_3^* = x_{30}^* - p_2 e_3 = \mathcal{Q} + P_m - p_2 e_3,\ c_2 > 0,\ 0 < p_2 < 1 \\ x_4^* = x_{40}^* - p_3 e_4 = \mathcal{Q} - p_3 e_4,\ 0 < p_3 < 1 \\ x_5^* = x_{50}^* - p_4 e_5 = \mathcal{Q} - p_4 e_5,\ 0 < p_4 < 1 \end{cases} \tag{8}$$

where $\mathcal{Q} = \frac{(1-p_1)M}{3}(c_2 e_2 + (1 - p_1)e_1 + c_1 x_2) - \frac{Dx_2}{3}$. Then it holds

$$\dot{V}_2 = -c_1 e_1^2 - c_2 e_2^2 - \frac{e_2}{(1 - p_1)M}\left[(1 - p_2)e_3 + (1 - p_3)e_4 + (1 - p_4)e_5\right] \tag{9}$$

Step 3: Now, in accordance with the sliding mode surface, the sliding mode surface σ_k is defined as follows:

$$\sigma_k = d_1 e_1 + d_2 e_2 + e_k, \quad k = 3, 4, 5 \tag{10}$$

where d_1 and d_2 are positive constants. Thus, the time derivative of the sliding surface is obtained as follows:

$$\dot{\sigma}_k = d_1\dot{e}_1 + d_2\dot{e}_2 + \dot{e}_k \tag{11}$$

where $\dot{e}_k$ can be straightforwardly computed as follows.

$$\dot{e}_3 = \dot{x}_3 - \dot{x}_3^* = \dot{x}_3 - \dot{x}_{30}^* + p_2\dot{e}_3 = \frac{1}{1 - p_2}\left[\dot{x}_3 - \dot{x}_{30}^*\right] \tag{12}$$

$$\dot{e}_4 = \dot{x}_4 - \dot{x}_4^* = \dot{x}_4 - \dot{x}_{40}^* + p_3\dot{e}_4 = \frac{1}{1 - p_3}\left[\dot{x}_4 - \dot{x}_{40}^*\right] \tag{13}$$

$$\dot{e}_5 = \dot{x}_5 - \dot{x}_5^* = \dot{x}_5 - \dot{x}_{50}^* + p_4\dot{e}_5 = \frac{1}{1 - p_4}\left[\dot{x}_5 - \dot{x}_{50}^*\right] \tag{14}$$

Thus, the augmented Lyapunov function with the sliding mode surface in (10) is obtained as follows:

$$V_3 = V_2 + \sum_{k=3}^{5}\sigma_k^2 \tag{15}$$

Subsequently, the time derivative of V_3 along the system trajectories (3) is given by

$$\begin{aligned}\dot{V}_3 &= \dot{V}_2 + \sigma_3\dot{\sigma}_3 + \sigma_4\dot{\sigma}_4 + \sigma_5\dot{\sigma}_5 \\ &= -c_1e_1^2 - c_2e_2^2 - \frac{e_2}{(1-p_1)M}((1-p_2)e_3 + (1-p_3)e_4 + (1-p_4)e_5) \\ &\quad + \sigma_3\left[d_1\dot{e}_1 + d_2\dot{e}_2 + \frac{1}{(1-p_2)}\left(f_3(x) + g_{31}(x)\frac{u_f}{T_0'} - \dot{x}_{30}^*\right)\right] \\ &\quad + \sigma_4\left[d_1\dot{e}_1 + d_2\dot{e}_2 + \frac{1}{(1-p_3)}\left(f_4(x) + g_{41}(x)\frac{u_f}{T_0'} + f_{42}(x)\frac{u_d}{T_d} - \dot{x}_{40}^*\right)\right] \\ &\quad + \sigma_5\left[d_1\dot{e}_1 + d_2\dot{e}_2 + \frac{1}{(1-p_4)}\left(f_5(x) + g_{51}(x)\frac{u_f}{T_0'} + f_{53}(x)\frac{u_q}{T_q} - \dot{x}_{50}^*\right)\right] \end{aligned} \tag{16}$$

Since $e_k = \sigma_k - d_1e_1 - d_2e_2$, $(k = 3, 4, 5)$, it is easy to compute the third term in (16) as follows.

$$\begin{aligned}\dot{V}_3 = &-\left(c_1 - \frac{(3-p_2-p_3-p_4)d_1}{M(1-p_1)}\right)e_1^2 - \left(c_2 - \frac{(3-p_2-p_3-p_4)(d_1+d_2)}{M(1-p_1)}\right)e_2^2 \\ &+ \sigma_3\underbrace{\left[d_1\dot{e}_1 + d_2\dot{e}_2 + \frac{1}{(1-p_2)}\left(f_3(x) + g_{31}(x)\frac{u_f}{T_0'} - \dot{x}_{30}^*\right) - \frac{(1-p_2)e_2}{(1-p_1)M}\right]}_{-\beta_3\sigma_3} \\ &+ \sigma_4\underbrace{\left[d_1\dot{e}_1 + d_2\dot{e}_2 + \frac{1}{(1-p_3)}\left(f_4(x) + g_{41}(x)\frac{u_f}{T_0'} + f_{42}(x)\frac{u_d}{T_d} - \dot{x}_{40}^*\right) - \frac{(1-p_3)e_2}{(1-p_1)M}\right]}_{-\beta_4\sigma_4} \\ &+ \sigma_5\underbrace{\left[d_1\dot{e}_1 + d_2\dot{e}_2 + \frac{1}{(1-p_4)}\left(f_5(x) + g_{51}(x)\frac{u_f}{T_0'} + f_{53}(x)\frac{u_q}{T_q} - \dot{x}_{50}^*\right) - \frac{(1-p_4)e_2}{(1-p_1)M}\right]}_{-\beta_5\sigma_5}\end{aligned} \tag{17}$$

where β_k, $(k = 3, 4, 5)$ are positive design parameters. Therefore, a suitable selection of the control law to accomplish the desired requirements is given as follows:

$$\begin{cases} u_f = -\dfrac{T_0'}{g_{31}(x)}\left[(1-p_2)\left(d_1x_2 + d_2\dot{e}_2 + \beta_3\sigma_3 - \dfrac{(1-p_2)e_2}{(1-p_1)M}\right) + f_3(x) - \dot{x}_{30}^*\right] \\ u_d = -\dfrac{T_d}{g_{42}(x)}\left[(1-p_3)\left(d_1x_2 + d_2\dot{e}_2 + \beta_4\sigma_4 - \dfrac{(1-p_3)e_2}{(1-p_1)M}\right) + f_4(x) + g_{41}(x)\dfrac{u_f}{T_0'} - \dot{x}_{40}^*\right] \\ u_q = -\dfrac{T_q}{g_{53}(x)}\left[(1-p_4)\left(d_1x_2 + d_2\dot{e}_2 + \beta_5\sigma_5 - \dfrac{(1-p_4)e_2}{(1-p_1)M}\right) + f_5(x) + g_{51}(x)\dfrac{u_f}{T_0'} - \dot{x}_{50}^*\right] \end{cases} \tag{18}$$

with $g_{31}(x) \neq 0$, $g_{42}(x) \neq 0$ and $g_{53}(x) \neq 0$.

4. **Closed-Loop Stability Analysis.** Now, we also need to analyze the closed-loop stability of the considered system with control law (18). We can summarize the developed control design above in the following theorem.

Theorem 4.1. *For the power system including SMES (3), the suitable design parameters* c_i, d_i, $(i = 1, 2)$, p_j, $(j = 1, 2, 3, 4)$ *are selected to meet the conditions:* $\bar{c}_1 = c_1 - \frac{(3-p_2-p_3-p_4)d_1}{M(1-p_1)} > 0$, $\bar{c}_2 = c_2 - \frac{(3-p_2-p_3-p_4)(d_1+d_2)}{(1-p_1)M} > 0$ *and* $\beta_k > 0$, $(k = 3, 4, 5)$ *are sliding mode gain coefficients. Subsequently, the improved backstepping sliding mode control law in (18) can guarantee that all trajectories of the system are bounded, and that the overall*

closed-loop error system (5), (7), (12)-(14) with the control law above is asymptotically stable.

Proof: After the proposed control law is obtained to stabilize the closed-loop system (3), we have

$$\dot{V}_3 = \dot{V}_2 + \sigma_3\dot{\sigma}_3 + \sigma_4\dot{\sigma}_4 + \sigma_5\dot{\sigma}_5 \leq -\bar{c}_1 e_1^2 - \bar{c}_2 e_2^2 - \sum_{k=3}^{5} \beta_k \sigma_k^2 \tag{19}$$

Additionally, it can be seen from (19) that $\dot{V}_3(t) \leq 0$. This implies that $V_3(t) \leq V_3(0)$, i.e., e_i, $(i = 1, 2, 3, 4, 5)$, σ_k, $(k = 3, 4, 5)$ are all bounded. We define

$$\mathcal{W}(t) = \bar{c}_1 e_1^2 + \bar{c}_2 e_2^2 + \sum_{k=3}^{5} \beta_k \sigma_k^2 \leq -\dot{V}_3(t) \tag{20}$$

Due to the fact that $V_3(0)$ is bounded and $V_3(t)$ is non-increasing and bounded, it can be concluded that

$$\lim_{t\to+\infty} \int_0^t \mathcal{W}(\tau)d\tau = \lim_{t\to+\infty} (V_3(0) - V_3(t)) < +\infty \tag{21}$$

Additionally, it can be observed from (20) that $\dot{\mathcal{W}}(t)$ is bounded and uniformly continuous. As a result, based on Barbalat's lemma [22], $\lim_{t\to+\infty} \mathcal{W}(t) = 0$ holds. Thus, with the help of the improved backstepping sliding mode strategy, we can conclude that $\lim_{t\to+\infty} e_i(t) = 0$ and $\lim_{t\to+\infty} \sigma_k(t) = 0$. From the definition of the system state variables x_i and x_i^*, $(i = 1, 2, 3, 4, 5)$, it is apparent that $x \to x_e$ as $t \to +\infty$. Finally, the overall closed-loop nonlinear system is asymptotically stable. This completes the proof.

Remark 4.1. *It is easy to observe that when $d_i = 0$, $(i = 1, 2)$, $p_j = 0$, $(j = 1, 2, 3, 4)$, the developed control law becomes the conventional backstepping control. Thus, the presented strategy can use the additional degrees of freedom in order to further enhance the desired control performances.*

Remark 4.2. *In contrast to the backsteppping sliding mode method presented in [16-19], the proposed scheme has the error compensation in the adverse effect of unknown error and can avoid the chattering problem arising from discontinuous control signals.*

Remark 4.3. *It can be observed that the proposed strategy is a systematic control strategy to design the desired control law by using three steps. The first two step is similar to the conventional backstepping strategy but adds some additional terms in the virtual control functions for error compensation. The final step is a suitable selection of the sliding mode surface to make the closed-loop system asymptotically stable. Further, the developed control law does not include the signum function unlike the control law reported in [16-19]. These make the proposed design procedure simpler than the I&I method and can improve the desired dynamic performances, simultaneously.*

5. **Simulation Results.** The presented control strategy is applied on a single-machine infinite bus (SMIB) power system with SMES whose schematic is shown in Figure 1. The desirable transient dynamic performances of the control system are illustrated to achieve the stability improvement of power angle and frequency regulation. Consider the SMIB model consisting of generator excitation and SMES which is connected through a parallel transmission line to an infinite bus. The MATLAB environment is used for the time-domain simulation of the control system under some conditions about the disturbances. Simulation studies are carried out for the power system under different contingencies.

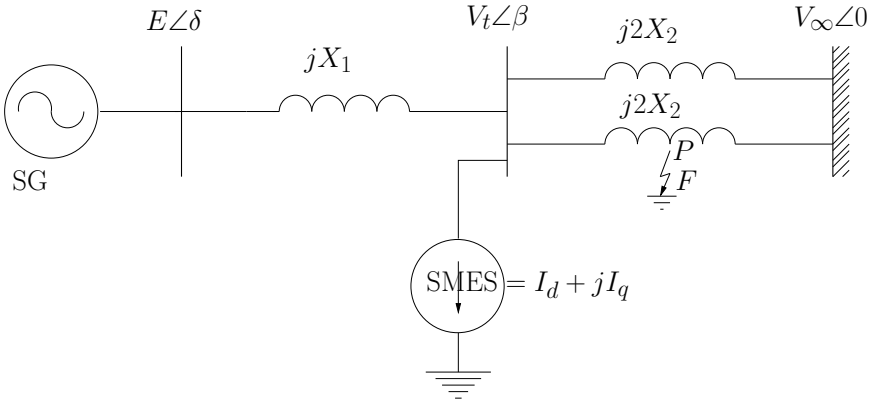

FIGURE 1. A single line diagram of SMIB model with SMES

In the simulations, the fault of interest is a symmetrical three phase short circuit occurring on one of the transmission lines as shown in Figure 1. The following two cases with a temporary fault sequence and a small perturbation to mechanical power to synchronous generators in the system are discussed.

Case 1: Effect of severe disturbance

Assume that there is a three-phase fault occurring at the point P (the middle of one of parallel transmission lines between the transformer and the infinite bus). Additionally, in this case, it is assumed that there are five stages of interest as follows. Firstly, all state variables are at pre-fault steady state. The fault occurs at $t = 0.5$ sec. After that, the breaker can isolate the fault at $t = 1.0$ sec. The transmission line can be restored at $t = 2.5$ sec. Eventually, the system returns to a post-fault state.

Case 2: Effect of small disturbance (small perturbation in mechanical power)

Similarly, in this case, it is assumed that there are three stages of interest as follows. First, the system is in a pre-fault steady state. Subsequently, there is a small constant perturbation in the mechanical power between $t = 0.5$ sec. and $t = 2.0$ sec. Afterward the system is in a post-fault state.

The simulation results are used to show the effectiveness of the developed method based on the following issues: (1) transient stability improvement and (2) power angle stability together with frequency and voltage regulation. Besides, the proposed scheme (18), i.e., the improved backstepping sliding mode control, is compared with the following two controllers.

- The immersion and invariance controller [12].

$$\begin{cases} u_f = \dfrac{T_f}{g_{31}(x)}\left[- f_3(x) + \dfrac{\partial \pi_3}{\partial x_1}\dot{x}_1 + \dfrac{\partial \pi_3}{\partial x_2}\dot{x}_2 - \gamma_1(x_3 - \pi_3(x_1, x_2))\right] \\ u_d = \dfrac{T_d}{g_{42}(x)}\left[- f_4(x) - g_{41}(x)\dfrac{u_f}{T_f} + \dfrac{\partial \pi_4}{\partial x_2}\dot{x}_2 - \gamma_2(x_4 - \pi_4(x_2))\right] \\ u_q = \dfrac{V_\infty T_q}{x_3 X_2}\left[- f_5(x) - \dfrac{x_5 V_\infty \sin x_1}{x_3 X'_{d\Sigma}}\dfrac{u_f}{T_f} + \dfrac{\partial \pi_5}{\partial x_2}\dot{x}_2 - \gamma_3(x_5 - \pi_5(x_2))\right] \end{cases} \tag{22}$$

where $\pi_3(x_1, x_2) = P_m + \beta M \sin x_{1e} + \gamma_d x_2 - \pi_4(x_2) - \pi_5(x_2)$, $\pi_4(x) = x_{4e} - \gamma_d x_2 = P_{de} - \gamma_d x_2$ and $\pi_5(x) = x_{5e} + \gamma_d x_2 = P_{qe} + \gamma_d x_2$, $\frac{\partial \pi_3}{\partial x_1} = \beta M \cos(x_1 - x_{1e})$, $\frac{\partial \pi_3}{\partial x_2} = -\frac{\partial \pi_4}{\partial x_2} = \frac{\partial \pi_5}{\partial x_2} = \gamma_d$. $\dot{x}_1$, $\dot{x}_2$ are given in (3). The control parameters are set as $\beta = 200$, $\gamma_d = 0.2$, $\gamma_i = 0.5$, $i = 1, 2, 3$.

- The conventional backstepping controller [22].

$$\begin{cases} u_f = -\dfrac{T_0'}{g_{31}(x)}\left[f_3(x) + c_3 e_3 + \dot{x}_{30}^* - \dfrac{e_2}{M}\right] \\ u_d = -\dfrac{T_d}{g_{42}(x)}\left[f_4(x) + g_{41}(x)\dfrac{u_f}{T_0'} + c_4 e_4 + \dot{x}_{40}^* - \dfrac{e_2}{M}\right] \\ u_q = -\dfrac{T_q}{g_{53}(x)}\left[f_5(x) + g_{51}(x)\dfrac{u_f}{T_0'} + c_5 e_5 + \dot{x}_{50}^* - \dfrac{e_2}{M}\right] \end{cases} \tag{23}$$

where $\dot{x}_{k0}^*$ are given in (12)-(14) and $c_i = 20$, $i = 1, 2, 3, 4, 5$.

The physical parameters (pu.) and initial conditions $(\delta_0, \omega_0, P_{e0}, P_{d0}, P_{q0})$ for this power system model are given in [12]. The tuning parameters of the proposed controller are $c_1 = c_2 = 20$, $d_1 = d_2 = 1$, $p_j = 0.5$, $(j = 1, 2, 3, 4)$. The SMIB power system consisting of generator excitation and SMES has been simulated using the the physical parameters and initial conditions above.

Remark 5.1. *It is observed in Theorem 4.1 that the developed control law depends upon the parameters p_i, d_1, d_2, c_1, c_2, and β_k. These tuning parameters of the proposed control are selected as follows. First of all, p_i is set as 0.5 because p_i needs to be selected between 0 and 1 $(0 < p_i < 1)$. For simplicity, d_1 and d_2 in (10) are chosen as 1. Subsequently, in order to make the closed-loop system stable, c_1 and c_2 are properly selected such that the following conditions (i) $\bar{c}_1 = c_1 - \frac{(3-p_2-p_3-p_4)d_1}{M(1-p_1)} > 0$, (ii) $\bar{c}_2 = c_2 - \frac{(3-p_2-p_3-p_4)(d_1+d_2)}{(1-p_1)M} > 0$, and (iii) sliding mode gains $\beta_k > 0$, $(k = 3, 4, 5)$, are all satisfied. Based on the suitable selection above, it can be seen in (19) that $\dot{V}_3 \leq 0$. This implies that $V_3(t) \leq V_3(0)$ i.e., e_i, $(i = 1, 2, 3, 4, 5)$, σ_k, $(k = 3, 4, 5)$ are all bounded. Finally, it is easy to conclude that the overall closed-loop system is asymptotically stable.*

The simulation results are presented and discussed below. In Case 1, Figures 2 and 3 illustrate time histories of power angle, frequency, active power, and terminal voltage, respectively. According to these figures, it is easy to see that the time trajectories can well track the reference and the tracking error eventually settles to zero. In addition, it can be seen in terms of transient behavior that the proposed method can provide the similar results as those of the I&I method. Also, the proposed strategy provides faster convergence and damping out power oscillations once compared with the results from the backstepping scheme. This can be used to confirm clearly that the developed control law achieves very good frequency and voltage regulation together with transient stability improvement according to the requirements mentioned previously. As shown in Figure 4 time trajectories of the sliding surface function can converge to zero as expected.

For Case 2, at the pre-fault steady state under the effect of a small perturbation of mechanical input power, it is assumed that there is a 30% perturbation $(\Delta P_m = 0.3 P_m)$ of mechanical input power. Figures 5 and 6 illustrate the time responses of power angle, frequency, active power, and terminal voltage. They obviously show the tracking performance superiority of the proposed over both the I&I method and the conventional backstepping method. Figure 7 illustrates time responses of the selected sliding surface function forced to zero, which shows the sliding surface described by $\sigma = 0$.

From figures, it can be seen that all time trajectories reach a steady-state condition, thereby exhibiting the closed-loop system stability. Additionally, the time responses of the presented controller are less oscillatory than the time responses given by the conventional backstepping controller, and are almost equal to those of the I&I controller. It is also evident that the performance of the conventional backstepping controller is the worst among the three methods. Therefore, the developed control provides significantly better

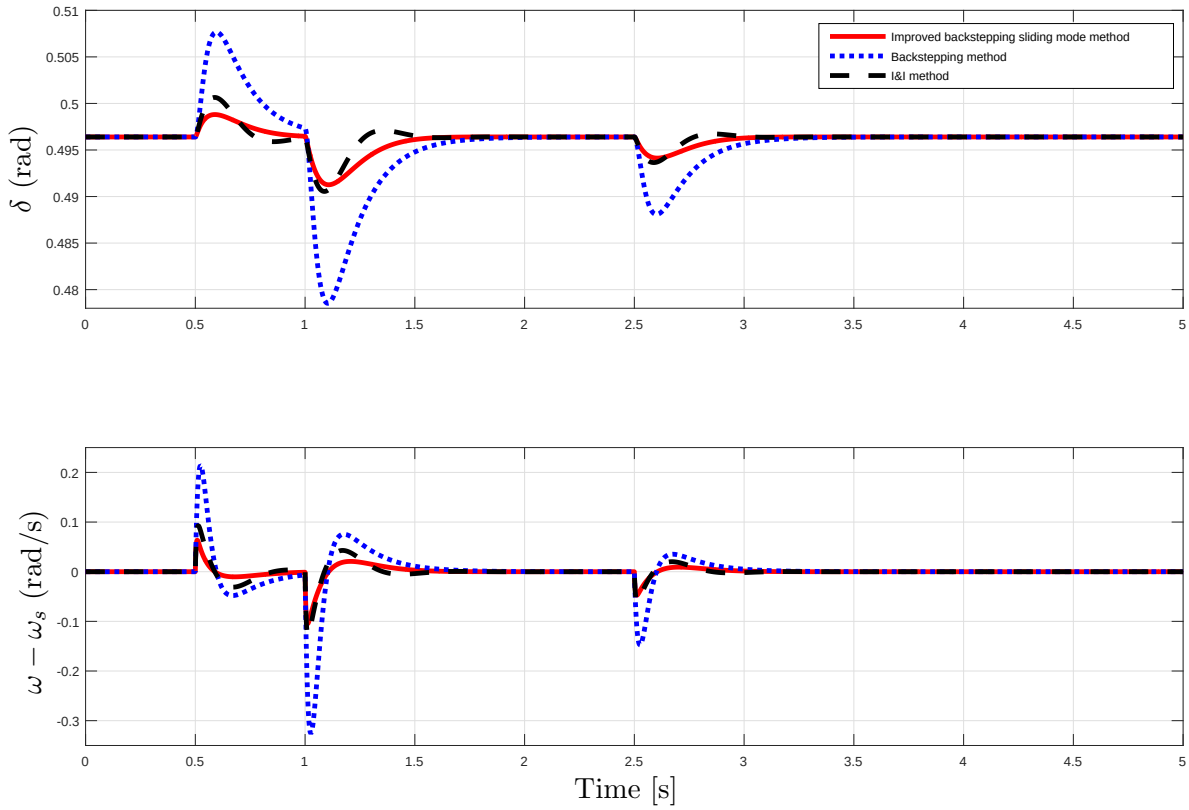

FIGURE 2. Case 1 – Time histories of power angle (δ) (deg.), and frequency ($\omega - \omega_s$) rad/s

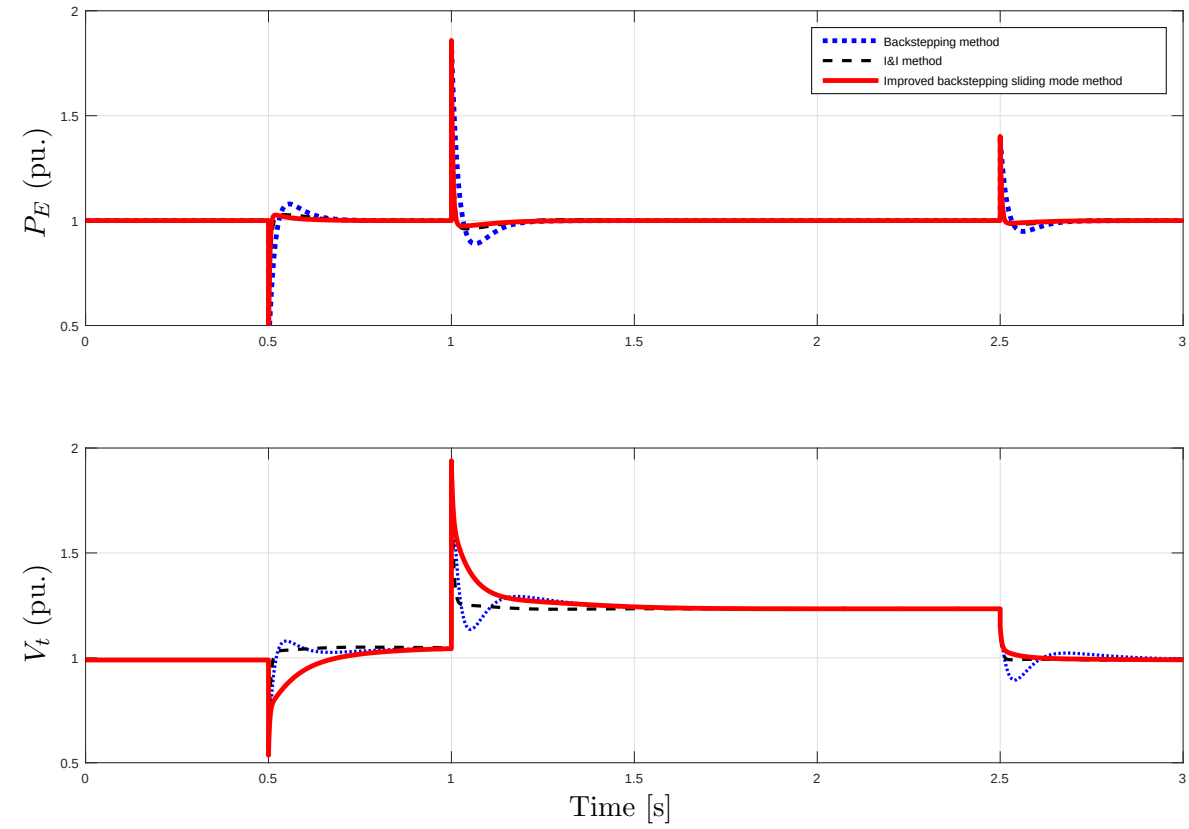

FIGURE 3. Case 1 – Time histories of active power (P_E) pu. and SMES terminal voltage (V_t) pu.

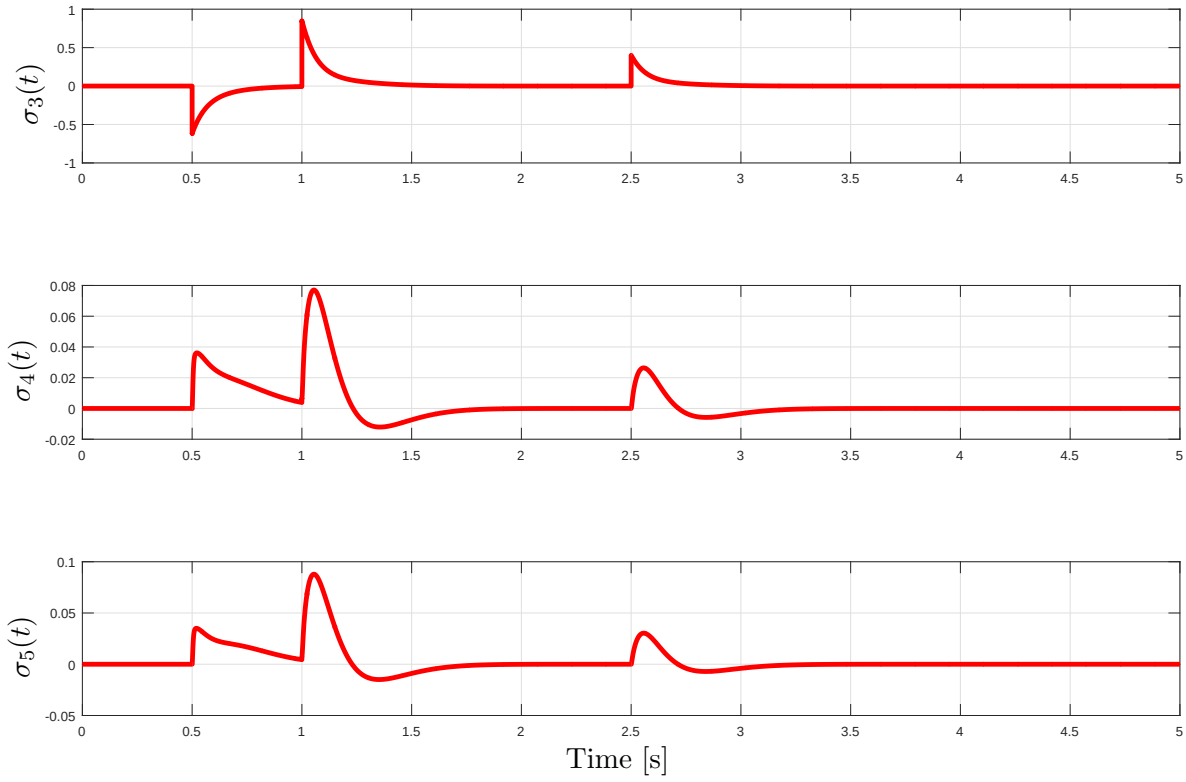

FIGURE 4. Case 1 – Time histories of sliding surface functions $\sigma_k(t)$, $k = 3, 4, 5$

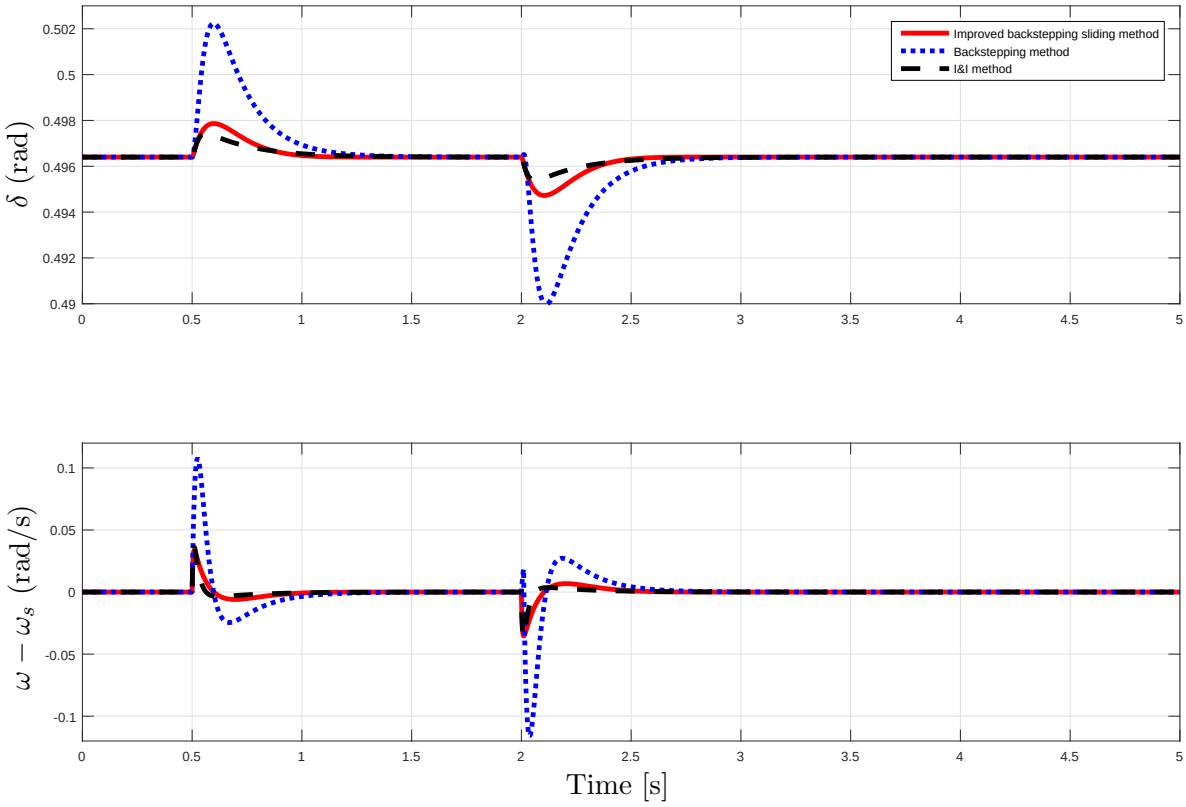

FIGURE 5. Case 2 – Time histories of power angle (δ) (deg.), and frequency ($\omega - \omega_s$) rad/s

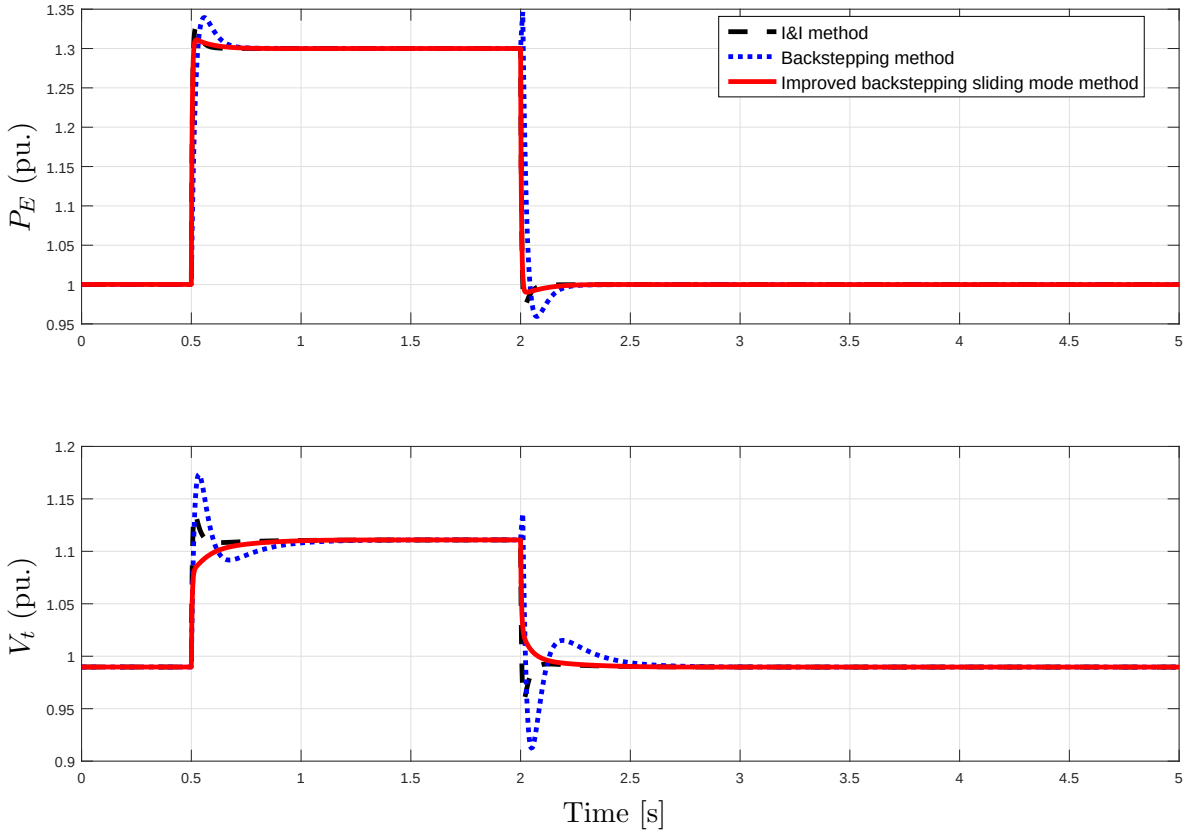

FIGURE 6. Case 2 – Time histories of active power (P_E) pu. and SMES terminal voltage (V_t) pu.

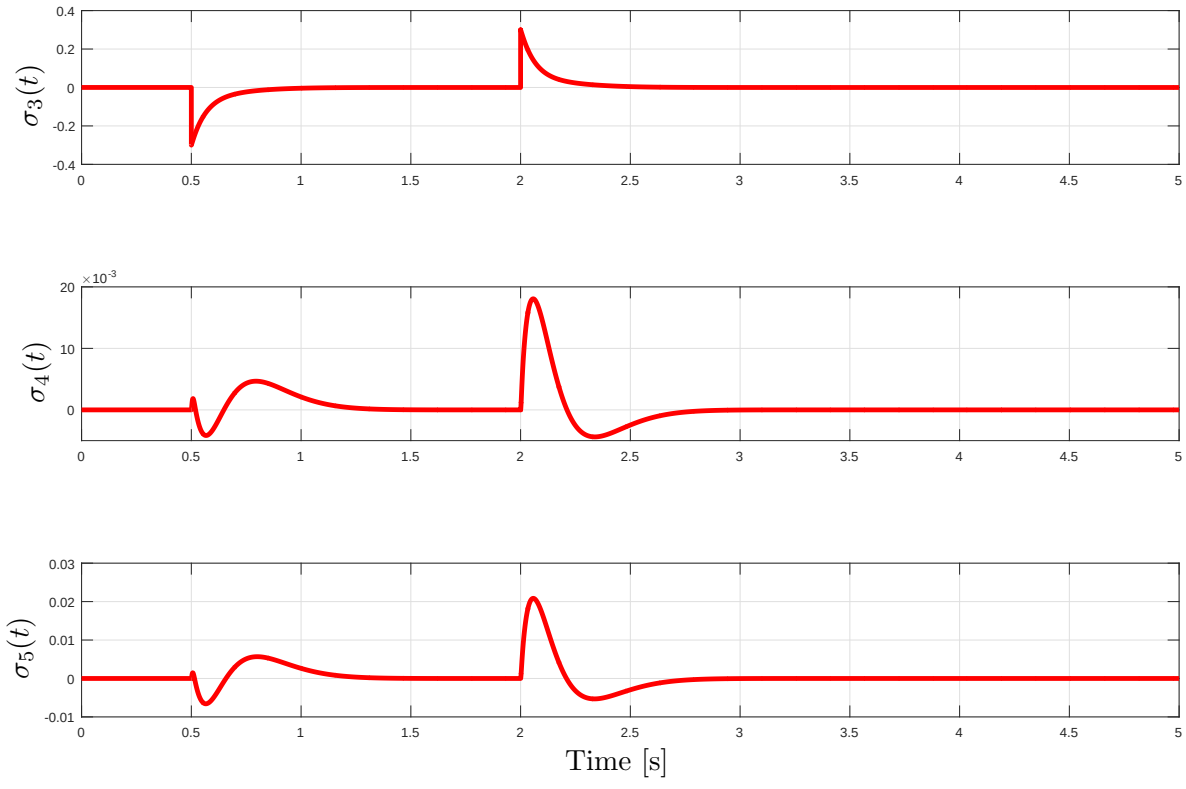

FIGURE 7. Case 2 – Time histories of sliding surface functions $\sigma_k(t)$, $k = 3, 4, 5$

damping enhancement in the power oscillation. Further, it is easy to observe that the overshoot magnitude, rise time, and settling time are clearly reduced. In this case, it can be concluded that the time responses of both the I&I control and the presented one, provide the similar results. Nevertheless, the proposed scheme is simpler design procedure than the I&I scheme.

From the simulation results with two different cases, it can be, overall, concluded that the proposed control law can be applied for transient stabilization and voltage regulation following small and large disturbances. The developed control strategy can make the closed-loop dynamic behaviors of the system converge quickly to a desired equilibrium point almost similar to the I&I design. Meanwhile, the time responses of all trajectories can quickly settle to the steady-state value condition. Despite the simple proposed design procedure, the time trajectories of the proposed scheme are almost similar to those of the I&I one. Further, it obviously outperforms the conventional backstepping one in terms of damping enhancement in the power oscillation together with smaller overshoot magnitude and shorter settling time.

6. **Conclusion.** In this work, the proposed nonlinear control law has been constructed via the improved backstepping sliding mode strategy for transient stability enhancement and voltage regulation of a single-machine infinite bus power system with superconducting magnetic energy storage system. The simulation results have shown that the developed control method is evaluated under large and small disturbances in the power systems and can stabilize the power angle, terminal voltage, and frequency. From the developed design procedure, it can be seen that the presented scheme is obviously simpler than the I&I one. It also provides good transient control performance similar to the I&I control and performs better than the conventional backstepping control. Moreover, the comparative results confirm the effectiveness of the proposed controller over the backstepping one in damping power oscillations in the closed-loop system dynamics, improving voltage and frequency regulation, and enhancing transfer capability. Future study will be devoted to extension of this approach to a robust adaptive control design in the presence of disturbance and unknown parameters.

REFERENCES

[1] P. Ribeiro, B. Johnson, M. L. Crow, A. Arsoy and Y. Liu, Energy storage systems for advanced power applications, *Proc. of IEEE*, vol.89, pp.1744-1756, 2000.

[2] A. H. Ali, B. Wu and R. A. Dougal, An overview of SMES applications in power and energy systems, *IEEE Trans. Sustainable Energy*, vol.1, pp.38-47, 2010.

[3] C.-F. Lu, C.-C. Liu and C.-J. Wu, Dynamic modelling of battery energy storage system and application to power system stability, *IEE Proceedings – Generation, Transmission and Distribution*, vol.142, pp.429-435, 1995.

[4] S.-K. Kim, H. Song and T.-W. Yoon, Damping improvement and terminal voltage regulation for a synchronous machine using an energy storage device, *International Journal of Electronics*, vol.102, pp.582-598, 2015.

[5] Y. Wang, G. Feng, D. Cheng and Y. Liu, Adaptive $\mathcal{L}_2$ disturbance attenuation control of multi-machine power systems with SMES units, *Automatica*, vol.42, pp.1121-1132, 2006.

[6] Y. Wan and J. Zhao, Extended backstepping method for single-machine infinite-bus power systems with SMES, *IEEE Trans. Control Systems Technology*, vol.21, pp.915-923, 2013.

[7] Y.-L. Tan and Y. Wang, A robust nonlinear excitation and SMES controller for transient stability, *International Journal of Electrical Power Energy Systems*, vol.26, pp.325-332, 2004.

[8] Y.-L. Tan and Y. Wang, Augmentation of transient stability using a superconducting coil and adaptive nonlinear control, *IEEE Trans. Power Systems*, vol.13, pp.361-366, 1998.

[9] F. Liu, S. Mei, D. Xia, D. Ma, X. Jiang and Q. Lu, Experimental evaluation of nonlinear robust control for SMES to improve the transient stability of power systems, *IEEE Trans. Energy Conversion*, vol.19, pp.774-782, 2004.

[10] S. Li and Y. Wang, Robust adaptive control of synchronous generators with SMES unit via Hamiltonian function method, *International Journal Systems Science*, vol.38, pp.187-196, 2007.
[11] M. A. Mahmud, M. J. Hossain and H. R. Pota, Dynamical modeling and nonlinear control of superconducting magnetic energy systems: Applications in power systems, *Australasian University Power Energy Conference*, Perth, Australia, 2014.
[12] A. Kanchanahanathai, V. Chankong and K. A. Loparo, Nonlinear generator excitation and superconducting magnetic energy storage control for transient stability enhancement via immersion and invariance, *Transactions of the Institute of Measurement and Control*, vol.37, no.10, pp.1217-1231, 2015.
[13] A. Astolfi and R. Oreta, Immersion and invariance: A new tool for stabilization and adaptive control of nonlinear systems, *IEEE Trans. Automatic Control*, vol.48, pp.590-606, 2003.
[14] A. Astolfi, D. Karagiannis and R. Ortega, *Nonlinear and Adaptive Control Design with Applications*, Springer-Verlag, 2007.
[15] A. Kanchanahanathai and E. Mujjalinvimut, Application of adaptive synergetic control to power systems with superconducting magnetic energy storage system, *International Journal of Innovative Computing, Information and Control*, vol.13, no.6, pp.1873-1885, 2017.
[16] K. Dahech, M. Allouche, T. Damak and F. Tadeo, Backstepping sliding mode control for maximum power point tracking of a photovoltaic system, *Electric Power Systems Research*, vol.143, pp.182-188, 2017.
[17] N. Adhakary and C. Mahanta, Integral backstepping sliding mode control for underactuated systems: Swing-up and stabilization of the cart-pendulum system, *ISA Transactions*, vol.52, pp.870-880, 2013.
[18] T. Espinoza, A. E. Dzul, R. Lozano and P. Parada, Backstepping – Sliding mode controllers applied to a fixed-wind UAV, *Jounal of Inteligent Robotic Systems*, vol.73, pp.67-79, 2014.
[19] F.-J. Lin, P.-H. Shen and S.-P. Hsu, Adaptive backstepping sliding mode control for linear induction motor drive, *IEE Proceedings – Electronic Power Applications*, vol.149, pp.184-194, 2002.
[20] Q. Su, W. Quan, G. Cai and J. Li, Improved adaptive backstepping sliding mode control for generator steam valves of nonlinear power systems, *IET Control Theory & Applications*, vol.11, no.9, pp.1414-1419, 2017.
[21] Q. Su, W. Quan, G. Cai and J. Li, An improved adaptive backstepping approach on static var compensator controller of nonlinear power systems, *International Journal of Adaptive Control and Signal Processing*, vol.32, pp.700-712, 2018.
[22] M. Krstic, I. Kanellakopoulos and P. V. Kokotivic, *Nonlinear and Adaptive Control Design*, John Willey & Sons, 1995.